Talanta 81 (2010) 1454–1460

Contents lists available at ScienceDirect

Talanta

journal homepage: www.elsevier.com/locate/talanta

Macroporous silica for concentration of nitroenergetic targets

Brandy J. Johnson[a,*,1], Brian J. Melde[a], Paul T. Charles[a], Michael A. Dinderman[a], Anthony P. Malanoski[a], Iwona A. Leska[b], Syed B. Qadri[c]

[a] Center for Bio/Molecular Science & Engineering, Naval Research Laboratory, Washington, DC 20375-5348, United States
[b] NOVA Research Incorporated, Alexandria, VA 22308, United States
[c] Materials Science and Technology Division, Naval Research Laboratory, Washington, DC 20375-5348, United States

ARTICLE INFO

Article history:
Received 23 December 2009
Received in revised form 17 February 2010
Accepted 18 February 2010
Available online 25 February 2010

Keywords:
Macroporous monolith
Periodic mesoporous organosilica
Hierarchical material
Solid phase extraction
TNT
RDX

ABSTRACT

Hierarchical organosilicate sorbents were synthesized which possess structure on two length scales: macropores of approximately 1 μm lined by mesopores (35–45 Å). The incorporation of macropores provides enhanced flow-through characteristics over purely mesoporous materials, thereby reducing back pressure when used in column formats. Materials of this type with varied surface groups were applied to the adsorption of 2,4,6-trinitrotoluene (TNT) and 1,3,5-trinitro-1,3,5-triazacyclohexane (RDX) in both batch and column formats. The results presented here demonstrate the potential of these materials for application as solid phase extraction materials for the pre-concentration of nitroenergetic targets from aqueous solutions. The structural and binding characteristics of the materials have been evaluated and preliminary data on the impact of complex matrices is provided.

Published by Elsevier B.V.

1. Introduction

RDX (hexahydro-1,3,5-trinitro-1,3,5-triazine), HMX (octahydro-1,3,5,7-tetranitro-1,3,5,7-tetrazocine), and TNT (2,4,6-trinitrotoluene) as well as their associated breakdown products are present in the soil and groundwater at many U.S. Department of Defense testing and training facilities. Many of these compounds are suspected or confirmed carcinogens, and there is concern regarding their ecological impact. Monitoring the presence of such contaminants in the environment is challenging due to the rapid diffusion of targets into the surrounding matrix. Pre-concentration of targets is often necessary to provide levels that are detectable by currently available technologies. In addition, it is often desirable to remove non-target analytes from samples to prevent their interference with evaluation of targets.

Solid phase extraction (SPE) involves absorbing targets onto a functionalized solid support. Desorption of target is accomplished either through a thermal process or through elution from the support using a solvent. The absorption of targets may be through non-selective, semi-selective, or more specific binding mechanisms. Solid phase microextraction (SPME) is one example of this technique [2–5]. SPME uses chemically modified silica fibers with thermal desorption. The surface area of the sorptive material is low in these systems, and exhaustive extraction of targets generally requires prohibitively long incubation times [5]. Some efforts have focused on increasing the surface area available to this technique [6]. Other efforts have focused on reducing the fragile character of SPME fibers through the use of metals rather than silica [7]. Semi-permeable membrane devices (SPMD) represent another type of SPE material. SPMDs are passive integrative sampling devices that are often used to provide a time-weighted average concentration of contaminants. Like polyethylene (PEDs) and polyoxymethylene (POMs) devices, sorption occurs through partitioning [8–15]. The insensitivity of this approach to short-term variations in concentration can be either an advantage or disadvantage depending on the particular water monitoring application. Equilibration of these devices with environmental conditions often requires days to weeks.

Our efforts in developing SPE materials have focused on periodic mesoporous organosilicas (PMOs) which are hybrid

Abbreviations: SPE, solid phase extraction; SPME, solid phase microextraction; SPMD, semi-permeable membrane devices; PEDs, polyethylene devices; POMs, polyoxymethylene devices; PMOs, periodic mesoporous organosilicas; DEB, 1,4-bis(trimethoxysilylethyl)benzene; BTE, 1,2-bis(trimethoxysilyl)ethane; PTS, phenyltrimethoxysilane; TMB, mesitylene; BET, Brunauer–Emmett–Teller; BJH, Barrett–Joyner–Halenda; MM1, hierarchical sorbent material; P10, hierarchical sorbent material with surface terminal phenyl groups.

* Corresponding author at: Naval Research Laboratory, Center for Bio/Molecular Science & Engineering, 4555 Overlook Ave SW, Code 6900, Washington, DC 20375, United States. Tel.: +1 202 404 6100; fax: +1 202 767 9598.
E-mail address: brandy.white@nrl.navy.mil (B.J. Johnson).

[1] SDC approach for determining author sequence has been employed [1].

0039-9140/$ – see front matter. Published by Elsevier B.V.
doi:10.1016/j.talanta.2010.02.050

organic/inorganic materials synthesized by condensing organic-bridged multifunctional silanes around surfactant micelles [16–19]. The materials possess high surfaces areas with the rugged character of silicates and the binding characteristics expected of organic functional groups. We have previously described the synthesis of ordered and semi-ordered organosilicate materials and their application to the adsorption of nitroenergetic compounds [20]. These materials were synthesized through co-condensation of 1,4-bis(trimethoxysilylethyl)benzene (DEB) and 1,2-bis(trimethoxysilyl)ethane (BTE) in the presence of Brij®76 micelles. We were able to demonstrate enhanced order through the use of co-condensation as well as enhanced selectivity through the use of a templating process involving the incorporation of 3,5-dinitrobenzoyl modified Brij®76. The modified surfactant provided a target-like structure in contact with the pore walls during condensation. The study focused on optimizing components of the synthesis to provide ordered, semi-selective sorbents for application to 2,4,6-trinitrotoluene (TNT) and dinitrotoluene (DNT) targets in aqueous samples.

While the materials developed in the previous study provided the desired binding characteristics, application of the sorbents was limited by the structural characteristics. The particle sizes in the PMO powders are small resulting in dense packing within a column; there may be poor interconnectivity between the pores throughout a given particle; the pore sizes within the particles are on the order of 30 Å. These aspects combine to produce poor performance in a column format due to the generation of high back pressures. The use of a column format is desirable when designing a system for in-line pre-concentration of targets. One method for reducing the back pressure is to mix these materials with sand or other materials of a controlled larger particle size. This allows for application in column formats; however, it also reduces the capture surface area in the column. In addition, the PMO materials eventually compact to the end of the column resulting in increasing back pressure. In order to address the high back pressures generated by the sorbents, we combined lessons learned through the development of the mesoporous sorbents with a method for the synthesis of monolithic organosilicates employing Pluronic P123 to template the mesostructures. This new method produces a hierarchical material with mesopores organized within macropores. The larger pores provide reduced pressure and increased connectivity and flow. The mesostructure provides the desired high concentration of binding sites. Here, we describe the hierarchical materials and demonstrate their potential for application to the pre-concentration of nitroenergetic targets for the enhancement of detection applications.

2. Experimental

2.1. Reagents

Phenyltrimethoxysilane (PTS), 1,4-bis(trimethoxysilylethyl) benzene (DEB) and 1,2-bis(trimethoxysilyl)ethane (BTE) were obtained from Gelest, Inc. (Tullytown, PA). NaOH, HCl, 3,5-dinitrobenzoyl chloride ≥98%, dichloromethane (≥99.5%), magnesium turnings (98%), p-cresol (pCr), and p-nitrophenol (pNP) were purchased from Sigma–Aldrich (St. Louis, MO). The activated charcoal used here for comparison purposes was purchased from Sigma–Aldrich (catalog #05113). Nitrogen sorption for this product was used to determine a BET surface area of 905 m^2/g and a BJH pore volume of 0.432 cm^3/g. Pluronic P123 (referred to here as P123) was a gift from BASF (Mount Olive, NJ). 2,4,6-Trinitrotoluene (TNT), hexahydro-1,3,5-trinitro-1,3,5-triazine (RDX), nitroglycerin (NG), and 2,4-dinitrotoluene (DNT) were purchased from Cerilliant (Round Rock, TX). Water was deionized to 18.2 MΩ cm using a Millipore Milli-Q UV-Plus water purification system. Artificial sea water was prepared using sea salts as directed by the supplier (Sigma–Aldrich). Pond water samples were collected from a park in Alexandria, VA, USA.

2.2. Materials synthesis and imprint template

Synthesis of the hierarchical material referred to as MM1 was accomplished using a variation on our previously reported technique [20,21]: 1.66 g P123 was combined with 0.24 g 3,5-dinitrobenzoyl modified P123 (described below) and dissolved with 0.2 g mesitylene (TMB) in 6 g of 0.1 M HNO_3 with stirring at 60 °C. The stirring solution was allowed to cool to room temperature, and a siloxane mixture consisting of 7.84 mmol total bis-silane (BTE + DEB at a molar ratio of 1 to 1) was added drop wise. The reaction mixture was stirred until homogeneous and transferred to a culture tube which was sealed tightly and heated at 60 °C over night (approximately 18 h). A white gel formed during this period. The tube was unsealed and heated at 60 °C for 2 days followed by incubation at 80 °C for an additional 2 days. The product, in the form of a white monolith, was refluxed three times in ethanol for at least 12 h to extract P123. This process broke the monolith producing a powder. The powder was collected by suction filtration, rinsed with ethanol and water, and dried at 100 °C. Synthesis of a sorbent material with terminal phenyl groups (P10) and no imprint employed a similar protocol using variations on the constituent concentrations. Pluronic P123 (1.9 g) was dissolved with 0.55 g mesitylene (TMB) in 7.5 g of 0.1 M HNO_3. Phenyltrimethoxysilane was incorporated into the material to provide enhanced functionality through the use of a siloxane mixture consisting of 7.84 mmol total silane with a BTE:DEB:PTS molar ratio of 50:40:10.

The imprint template for the materials was prepared by esterification of Pluronic P123 with 3,5-dinitrobenzoyl chloride. This was accomplished as follows [20]: 8 g P123, 1.27 g 3,5-dinitrobenzoyl chloride, and magnesium turnings were added to 60 mL dichloromethane and refluxed for 2 h. The solution was shaken with 60 mL 2% aqueous $NaHCO_3$. The organic phase was collected and evaporated to yield the yellow, derivatized surfactant.

2.3. Characterization methods

A Micromeritics ASAP 2010 was used for N_2 sorption experiments performed at 77 K. Prior to analysis, samples were degassed to 1 μm Hg at 100 °C. Standard methods were applied to the calculation of characteristics. Surface area was determined by use of the Brunauer–Emmett–Teller (BET) method; pore size was calculated by the Barrett–Joyner–Halenda (BJH) method from the adsorption branch of the isotherm; total pore volume was calculated by the single point method at relative pressure (P/P_0) 0.97. Thermogravimetric analysis was performed using a TA Instruments Hi-Res 2950 Thermogravimetric Analyzer under a N_2 atmosphere; temperature was ramped 5 °C/min to 800 °C. Powder X-ray diffraction patterns were obtained with a Rigaku high-resolution powder diffractometer with 18 kW CuKα radiation derived from a high-power Rigaku rotating anode X-ray generator.

Conducting carbon tape was used to mount samples on SEM stubs for imaging by scanning electron microscopy (SEM). Sputter coating with gold under argon was accomplished using a Cressington 108 auto sputter coater for (duration 60 s). Scanning electron micrographs of the samples were collected using a LEO 1455 SEM (Carl Zeiss SMT, Inc., Peabody, MA). For imaging via transmission electron microscopy (TEM), samples were deposited onto a holey carbon grid (200 mesh copper, SPI, West Chester, PA) and viewed under an energy filtering transmission electron microscope (LIBRA 120 EFTEM, Carl Zeiss SMT, Peabody, MA) operated at 120 kV. Zero Loss, brightfield, energy filtered (EF) TEM images were captured on a bottom-mounted, digital camera (KeenView, Olympus SIS, Montvale, NJ).

2.4. Sorption experiments

HPLC analysis of samples was carried out on a Shimadzu High Performance Liquid Chromatography (HPLC) system with dual-plunger parallel flow solvent delivery modules (LC-20AD) and an auto-sampler (SIL-20AC) coupled to a photodiode array detector (SPD-M20A). A modification of EPA method 8330 was employed. The stationary phase was a 250 mm × 4.6 mm Altech Alltima C18 (5 μm) analytical column. An isocratic 50:50 methanol:water mobile phase was employed. A 20 μL sample injection was used with a flow rate of 1.3 mL/min. Sample solutions were in water, methanol, or acetonitrile as indicated. UV/vis detection of targets was accomplished at 254 nm.

Two types of experiments were used to characterize the binding capacity and affinity of the materials synthesized. Batch experiments were conducted in 20 mL scintillation vials (EPA Level 3; clear borosilicate glass; PTFE/silicone-lined cap). A fixed mass of sorbent (approximately 15 mg) was weighed directly into the vial using an analytical balance. Target samples were prepared in 18 MΩ Milli-Q deionized water unless otherwise indicated. Sample volumes were 20 mL unless otherwise indicated. Target solutions were added to the sorbents in the vials with a portion of the sample retained for use as a control during HPLC analysis. A series dilution of the retained sample was prepared for generation of a standard curve allowing for analysis of target binding by the sorbents. The vials were incubated overnight (unless otherwise indicated) on rotisserie mixers. Following incubation, samples were filtered using 25 mm Acrodisc 0.2 μm syringe filters with PTFE membranes. The filtered solutions were analyzed by HPLC, and difference method analysis was applied to determine the target removed from solution. Columns of the sorbent materials were prepared in BioRad disposable polypropylene columns using 200 mg of sorbent. Both gravity flow and controlled flow (4 mL/min) experiments were conducted. Controlled flow was accomplished using a peristaltic pump. As with batch experiments, HPLC difference analysis was used to determine target bound. Elution from the columns was accomplished using acetonitrile or methanol. LiChrolute EN (VWR International) and SepPak RDX (125–150 μm; Waters Corporation, Milford, MA) materials were handled identically to the sorbents prepared in-house.

3. Results and discussion

3.1. Material characteristics

Fig. 1 presents the SEM and TEM images of the MM1 hierarchical material. In the SEM image, pores of approximately 1 μm were clearly visible. The TEM image showing bands of lighter and darker regions is indicative of ordered pore structure. The XRD spectrum (Fig. 1) further confirmed the presence of ordered pores.

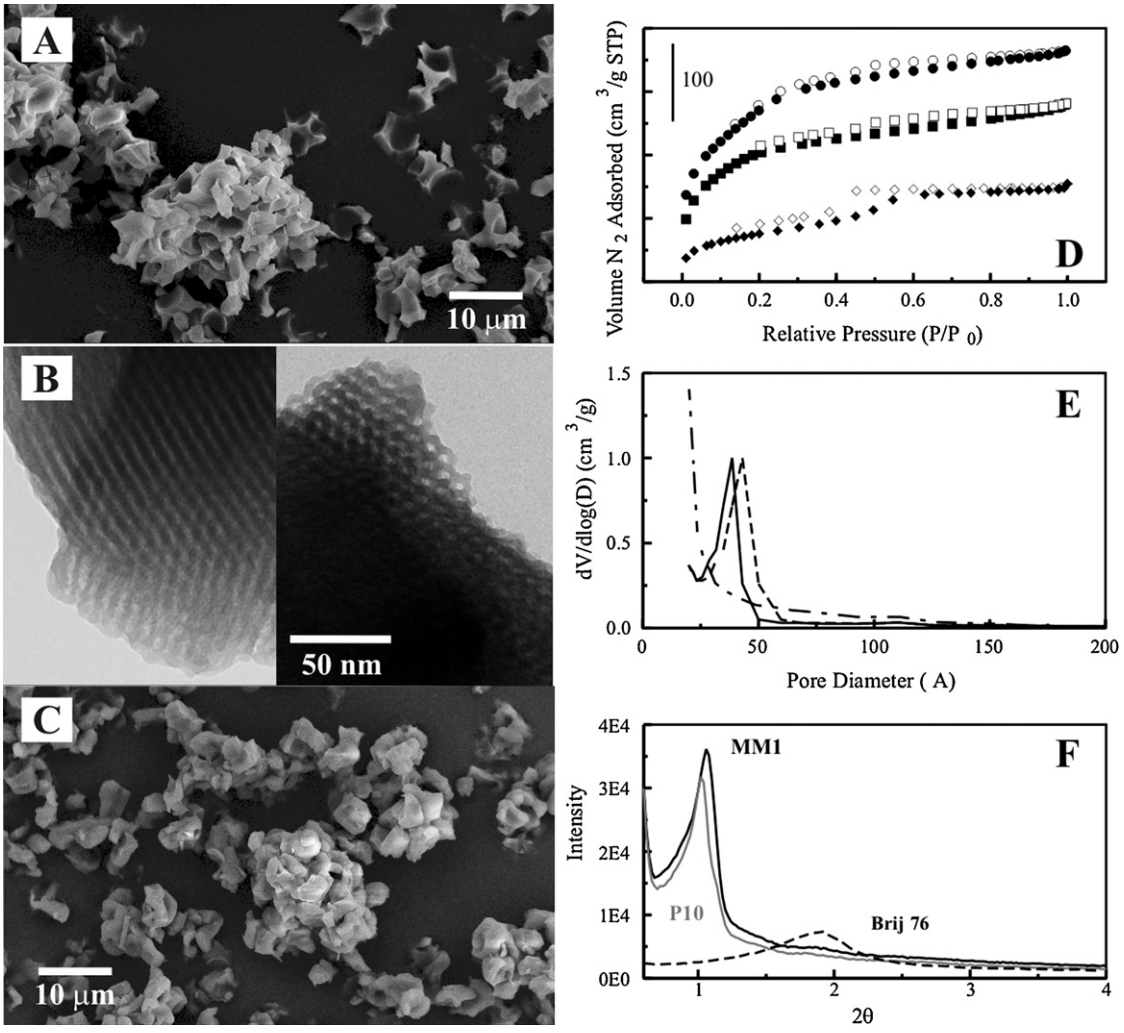

Fig. 1. Materials characteristics. Shown here are SEM (Panel A) and TEM (Panel B) images of MM1 and an SEM image of P10 (Panel C). Also presented are the nitrogen sorption isotherms (Panel D) for MM1 (circles), P10 (squares), and the 50:50 BTE:DEB material synthesized using Brij®76 (diamonds). Open symbols are for desorption, and filled symbols are for sorption. The pore diameter distributions (Panel E) and XRD spectra (Panel F) are presented for MM1, P10, and the 50:50 BTE:DEB material synthesized using Brij®76.

Here, the sharp profile of the primary reflection, as well as the presence of additional reflections in the spectrum, indicated increased mesoscale order over our previously reported materials. Increased order on the mesoscale generally provides improved access to the pore surfaces throughout the material. This increased order was interesting considering the concentration of DEB in MM1. For our previously reported materials, using 50% DEB with 50% BTE resulted in poor materials characteristics (Fig. 1) and a low degree of order. Nitrogen sorption analysis of MM1 yielded a type IV/type I isotherm common to mesoporous materials with uniform pore sizes (Fig. 1). As expected, the surface area of MM1 (366 m^2/g) was reduced as compared to the mesoporous material prepared with the same constituents (813 m^2/g). Mesopore volume was also reduced (from 0.46 to 0.26 cm^3/g for MM1), while the average pore size diameter was increased (from microporous to 35 Å for MM1).

Incorporation of terminal phenyl groups into the hierarchical material required a variation of the synthesis used for MM1. The resulting materials had reasonable materials characteristics, but were missing the macroporous characteristics observed for MM1. An SEM image of P10 is presented in Fig. 1. The open network of micron sized pores observed for MM1 was not seen in the SEM of P10. TEM imaging did not reveal ordered pores on the mesoscale. Nitrogen sorption analysis of P10 yielded a type IV/type I isotherm with surface area 276 m^2/g, pore volume 0.226 cm^3/g, and average pore diameter 43 Å. The XRD spectrum for P10 is presented in Fig. 1.

3.2. Batch sorption experiments

Standard binding isotherms for the binding of RDX and TNT by P10 and MM1, respectively, are presented in Fig. 2. The binding kinetics for the hierarchical materials were slower than expected (Fig. 2). We previously reported more than 90% of target bound in less than 5 min for mesoporous materials [20]. Using 15 mg of sorbent in 30 μM target (20 mL), we found that 20 min was required to achieve 95% of maximal target binding. The reasons for the change in rate were unclear. A larger, more open pore network would be expected to facilitate diffusion into the pores. Analysis of binding site homogeneity was conducted based on the method of Ockrent [22] and Weber [23]. TNT and RDX binding (for MM1 and P10, respectively) in the presence of p-cresol was evaluated (Fig. 2). Sample volume (20 mL), sorbent concentration (15 mg), and total target concentration (22 μM) were held constant while the ratio of p-cresol to TNT or RDX was varied. These types of studies tend to indicate whether non-targets will interfere with binding of targets or whether two targets bind to similar sites within the pores. When the evaluated targets bind to the same sites, this plot is typically linear. When targets are bound by differing sites, there is divergence from the line. On the basis of this data, it appears unlikely that compounds with structures similar to p-cresol will compete with targets (TNT or RDX) for binding sites. The semi-selectivity of MM1 was expected based on the results previously obtained for imprinted mesoporous materials.

TNT, DNT, RDX, nitroglycerin, and 2,4-dinitrotoluene are commonly found as co-contaminants. Additional competitive binding experiments were performed using mixtures of these targets (data provided in Supporting information). The concentrations used for these experiments are well below the binding capacity of the material for all of the evaluated targets. Binding of targets from solutions containing TNT and RDX indicated that these two targets are bound by differing sites within the materials under the evaluated conditions. Binding of TNT by MM1 from two component mixed solutions containing 2,4-dinitrotoluene (DNT), p-nitrophenol, or nitroglycerin indicated that these targets interact with the sites that bind TNT. TNT and DNT are of very similar structure, so their competition for sites is not unexpected. In order to understand the behavior of the other targets, it is important to note that, though imprinted,

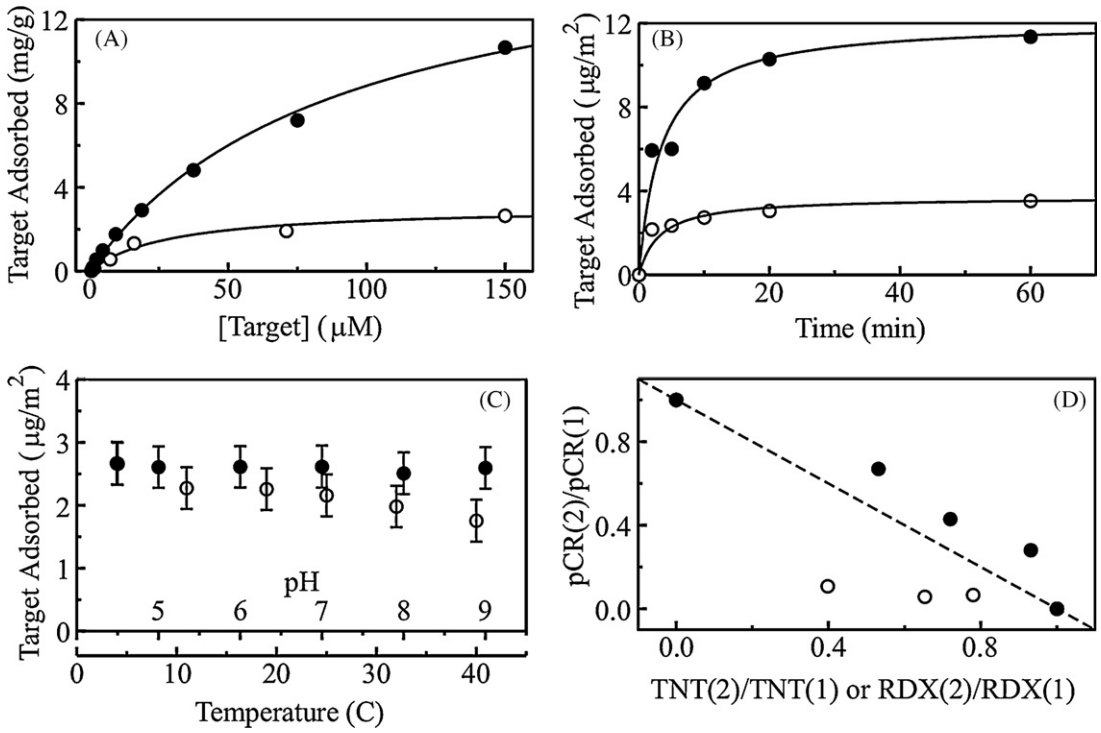

Fig. 2. Target binding. (A) Shown here are standard binding isotherms for TNT (solid) and RDX (open) by MM1 and P10, respectively. For these experiments, 15 mg of sorbent was placed in 20 mL of a target solution. (B) The kinetics for binding of TNT and RDX by MM1 (solid) and P10 (open), respectively, are shown here. For these experiments, 15 mg of sorbent was placed in a 20 mL sample containing 30 μM target in deionized water. (C) Altering the pH of samples (solid) through addition of phosphate buffer had little impact on the binding of TNT by MM1 while TNT binding decreased as the sample temperature increased (open). Here, 15 mg of sorbent was exposed to a 20 mL sample of 22 μM TNT. (D) The ratios of the targets bound from single (1) and multi-component (2) samples are plotted to provide an indication of binding site heterogeneity for MM1 (solid) and P10 (open). For these experiments, 15 mg of sorbent was exposed to 20 mL of a 22 μM total target solution where the ratio of p-cresol to TNT or RDX was varied.

the MM1 material is expected to have a distribution of heterogeneous binding sites for the target molecule. At low concentrations, TNT would be expected to interact primarily with the sites of highest affinity. As the concentration is increased, interaction with sites of lower affinity would also be expected. p-Nitrophenol is an aromatic ring bearing a nitro-group with structural similarity to TNT. Although nitroglycerin is a very different structure from the other three compounds, it has three nitro-groups linked by a flexible structure. While bearing three nitro-groups, the ring of RDX is more rigid than the nitroglycerin structure which may result in reduced affinity for the compound at the sites of high affinity for TNT. These results are valid under the conditions evaluated, however, competition for sites of lower TNT affinity would be likely at higher target loading levels.

In order to obtain a number indicative of affinity for these materials, linear fits for the double reciprocal form of binding isotherms collected at a constant target concentration of 22 μM were calculated. The data was fit using Langmuir–Freundlich model isotherms of the form:

$$q = \frac{q_s k[\mathrm{L}]^n}{1 + k[\mathrm{L}]^n} \quad (1)$$

This allowed for calculation of the saturation capacity (q_s) and the affinity coefficient (k) based on the concentration of unbound target ([L]) and the concentration of bound target (q). Here, n is the heterogeneity index (Table 1). We have applied this analysis to mesoporous materials in the past [20]. In those cases, reasonable fits were obtained when the heterogeneity index was held at unity. In the case of MM1, the heterogeneity index was not unity; it was 0.83 (Eq. (1)). This indicated that TNT was bound by sites of varying affinity. In the case of RDX binding by P10, a heterogeneity coefficient of 0.87 yielded a good fit. The TNT saturation capacity of MM1 was significantly higher than that reported for the mesoporous materials. The discrepancy between the saturation capacities for TNT and RDX was not unexpected. The diethylbenzene precursor was selected because of the π-bonds of the bridging group and the extension of those bonds into the electrical double layer. These π-bonds were expected to enhance interactions with TNT, but not necessarily with RDX. The difference in binding capacity is, therefore, likely due to the strong difference in the way these compounds interact with the functional groups within the sorbent. Further evidence of these differences was provided by the competitive binding data (above). TNT and RDX were not found to bind the same sites within the sorbent.

Table 1
Fit parameters and calculated characteristics from target binding isotherms.

	q_s (μg/m^2)	k (μg^{-1})
P10 (RDX)	3.3	0.046
MM1 (TNT)	70	0.003

Batch experiments were performed in artificial sea water and in pond water collected locally (Alexandria, VA) in order to obtain an idea of the potential for application of these materials to targets in complex matrices (Fig. 3). Water samples (20 mL) were spiked with 30 μM TNT or RDX. While the binding of TNT by MM1 was only slightly impacted by the pond water, the binding of RDX by P10 was completely abrogated in both of the matrices. This data indicates that P10 will likely not be useful for application outside of a laboratory situation. MM1 would be expected to perform under a range of different sample conditions. Binding of TNT by MM1 was evaluated at a range of pH values and at varying temperature (Fig. 2). The sample pH was altered using phosphate buffers (50 mM). Binding of TNT by MM1 was similar across the range of

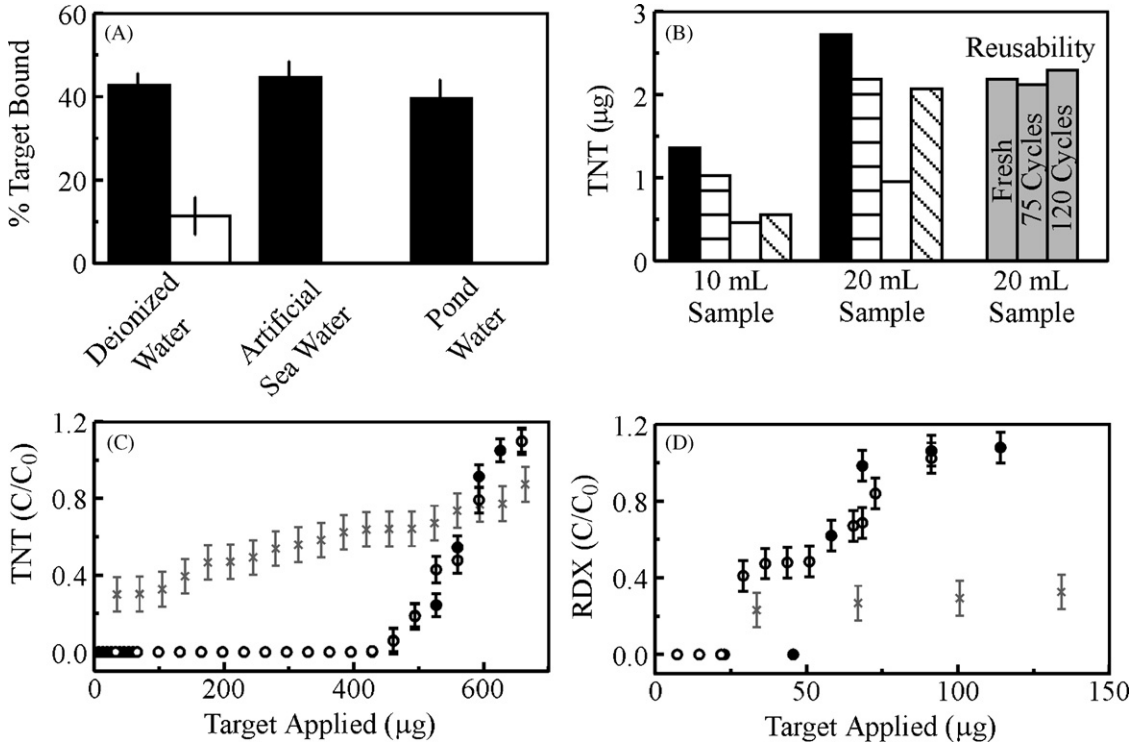

Fig. 3. Varied conditions. (A) Shown here is the percent target bound from 20 mL of a 30 μM solution of TNT (black) or RDX (white) by MM1 and P10, respectively. Target samples were prepared in deionized water, artificial sea water, and pond water. (B) The recovery of TNT bound by MM1 (horizontal lines) from a sample prepared in deionized water (100 ppb; 450 nM) is compared to that of Lichrolut EN (white) and SepPak (diagonal lines). The black bars show the total target applied. Also shown is the recovery under identical conditions using an MM1 column that was freshly prepared and after it was subjected to 75 and 120 capture/elution cycles (gray bars). (C) Shown here are TNT breakthrough curves for MM1 (solid), P10 (open), and activated charcoal (×). The TNT solution was prepared in deionized water. (D) Shown here are RDX breakthrough curves for MM1 (solid), P10 (open), and activated charcoal (×). The RDX solution was prepared in deionized water.

Table 2
Column format binding capacities.

Target	Material	Capacity		
		μg[a]	mg/g	μg/m^2
TNT	MM1	528	2.6	7.2
	P10	532	2.7	9.6
RDX	MM1	46	0.23	0.63
	P10	67	0.34	1.2

[a] In experiments employing a 200 mg column.

pH values evaluated (4.5–9.0). A decrease in the amount of TNT bound was noticed for increasing temperature. This is likely due to the decreased residence time of the target on the sorbent surface.

3.3. Column sorption experiments

MM1 and P10 were packed as 200 mg columns for evaluation of their potential for concentration of targets from dilute samples. The columns were characterized by measuring the breakthrough capacity and elution characteristics in comparison to activated charcoal as shown in Fig. 3. MM1 and P10 performed similarly in the column format. The total TNT binding capacities for the 200 mg columns were found to be approximately 530 μg (Table 2). The total RDX binding capacity was found to be nearly an order of magnitude lower (Table 2). Initial TNT breakthrough for P10 was noted at 400 μg (7.2 μg/m^2) and for MM1 at 450 μg (6.1 μg/m^2). Initial RDX breakthrough for P10 was noted at 25 μg (0.4 μg/m^2) and for MM1 at 50 μg (0.7 μg/m^2). Activated charcoal was used to provide a standard for comparison. The material was handled in the same manner as the other materials. Partial breakthrough for both targets was noted from the first application, but the total capacity was not reached for either target; a total of 700 μg was applied. Based on the calculations described above, TNT breakthrough on MM1 was expected at 5 mg. MM1 bound significantly less TNT than expected under the conditions used for the column experiments. P10 bound slightly less target than expected based on the calculations above.

MM1 was also compared to two commercially available preconcentration sorbents, LiChrolut EN and SepPak. As shown in Fig. 3, samples of either 10 mL or 20 mL of a 100 ppb TNT (450 nM) solution in deionized water were applied to 200 mg columns of each of the sorbents. No breakthrough was observed for any of the materials. Elution was accomplished using 1 mL of acetonitrile. Acetonitrile was selected as the eluant based on the directions provided for LiChrolut and SepPak. The concentration of the TNT recovered upon elution from MM1 was greater than that obtained from either of the other sorbents for both applied volumes. Elution of targets from MM1 was also possible using methanol with similar recovery. Fig. 3 also presents data demonstrating the reusability of the MM1 column. The recovery of TNT using MM1 is consistent whether the column is fresh or has been used for multiple capture/elution cycles.

4. Conclusions

Our previous efforts directed toward the development of sorbents for SPE of nitroenergetic targets were less than successful owing to the impracticality of their use in column formats. In order to address the excessive back pressure, we altered the synthesis of our previously described materials to include a larger surfactant combined with a swelling agent. These changes resulted in materials with order on two length scales. The mesopores were slightly larger than those of the earlier materials, and they were within macropores of about 1 μm. This approach sacrificed some of the surface area of the mesoporous materials, but it improved interconnectivity and access to the surface area. In fact, the saturation capacity of the hierarchical materials was greater than that of the earlier mesoporous materials. An additional hierarchical material was synthesized in which phenyltrimethoxysilane was used as 10% of the total precursor. This modification to the material was found to enhance RDX binding. Both MM1 (50:50, DEB:BTE material) and P10 (50:40:10, DEB:BTE:PTS) were evaluated for target extraction. While P10 was found to provide enhanced RDX capacity over MM1, it was also found that target binding was abrogated by complex matrices such as artificial sea water and pond water. The material was deemed unsuitable for application to real-world scenarios.

MM1 was compared to two commercially available resins described for the concentration of nitroenergetics. The material provided target concentrations in the eluate that were higher than those provided by either of the commercial polymer resins. In addition, a single column of MM1 was used for concentration of more than 120 samples from varying matrices with no loss of function. The material offers the potential for pre-concentration of targets in a reusable format applicable to situations such as long-term monitoring of energetic compounds contained in ground and surface waters near testing and training facilities. The material could be incorporated as an in-line concentrator for use with existent detection technologies. Alternatively, the material could be used for passive monitoring applications similar to those described for polyethylene devices [15].

Acknowledgements

This research was sponsored by the U.S. Naval Research Laboratory (NRL 6.1 WU#69-8765) and the U.S. DoD Strategic Environmental Research and Development Program (SERDP; ER-1604). We applied the SDC approach ("sequence-determines-credit") for determining the sequence of authors [1]. The views expressed here are those of the authors and do not represent those of the U.S. Navy, the U.S. Department of Defense, or the U.S. Government.

Appendix A. Supplementary data

Supplementary data associated with this article can be found, in the online version, at doi:10.1016/j.talanta.2010.02.050.

References

[1] T. Tscharntke, M.E. Hochberg, T.A. Rand, V.H. Resh, J. Krauss, PLoS Biology 5 (2007) e18.
[2] E.Y. Zeng, D. Tsukada, D.W. Diehl, Environmental Science & Technology 38 (2004) 5737–5743.
[3] J.M. Perr, K.G. Furton, J.R. Almirall, Journal of Separation Science 28 (2005) 177–183.
[4] F. Monteil-Rivera, C. Beaulieu, J. Hawari, Journal of Chromatography A 1066 (2005) 177–187.
[5] M.D. Engelmann, D. Hinz, B.W. Wenclawiak, Analytical and Bioanalytical Chemistry 375 (2003) 460–464.
[6] A. Gierak, M. Eredych, A. Bartnicki, Talanta 69 (2006) 1079–1087.
[7] D. Panavaite, A. Padarauskas, V. Vickackaite, Analytica Chimica Acta 571 (2006) 45–50.
[8] A.E. Vinturella, R.M. Burgess, B.A. Coull, K.M. Thompson, J.P. Shine, Environmental Science & Technology 38 (2004) 1154–1160.
[9] J.E. Tomaszewski, R.G. Luthy, Environmental Science & Technology 42 (2008) 6086–6091.
[10] M.T.O. Jonker, A.A. Koelmans, Environmental Science & Technology 35 (2001) 3742–3748.
[11] L. Hong, R.G. Luthy, Chemosphere 72 (2008) 272–281.
[12] F.A. Esteve-Turrillas, V. Yusa, A. Pastor, M. de la Guardia, Talanta 74 (2008) 443–457.
[13] G. Cornelissen, A. Pfttersen, D. Broman, P. Mayer, G.D. Breedveld, Environmental Toxicology and Chemistry 27 (2008) 499–508.
[14] M. Barthe, E. Pelletier, G.D. Breedveld, G. Cornelissen, Chemosphere 71 (2008) 1486–1493.
[15] R.G. Adams, R. Lohmann, L.A. Fernandez, J.K. Macfarlane, P.M. Gschwend, Environmental Science & Technology 41 (2007) 1317–1323.
[16] T. Asef, M.J. MacLachlan, N. Coombs, G.A. Ozin, Nature 402 (1999) 867–871.
[17] S. Inagaki, S. Guan, Y. Fukushima, T. Ohsuna, O. Terasaki, Journal of the American Chemical Society 121 (1999) 9611–9614.

[18] B.J. Melde, B.T. Holland, C.F. Blanford, A. Stein, Chemistry of Materials 11 (1999).
[19] C. Yoshina-Ishii, T. Asefa, N. Coombs, M.J. MacLachlan, G.A. Ozin, Chemical Communications (1999) 2539–2540.
[20] B.J. Johnson, B.J. Melde, P.T. Charles, D.C. Cardona, M.A. Dinderman, A.P. Malanoski, S.B. Qadri, Langmuir 24 (2008) 9024–9029.
[21] K. Nakanishi, Y. Kobayashi, T. Amatani, K. Hirao, T. Kodaira, Chemistry of Materials 16 (2004) 3652–3658.
[22] C. Ockrent, Journal of the Chemical Society (1932) 613–630.
[23] W.J. Weber, Journal of Applied Chemistry of the USSR 14 (1964) 565–572.